

## Chlorogenic Acid and Coffee Prevent Hypoxia-Induced Retinal Degeneration

Holim Jang,<sup>†,‡</sup> Hong Ryul Ahn,<sup>‡</sup> Hyoung Jo,<sup>‡</sup> Kyung-A Kim,<sup>‡</sup> Eun Ha Lee,<sup>‡</sup> Ki Won Lee,<sup>§</sup> Sang Hoon Jung,<sup>\*,‡,¶,||</sup> and Chang Y. Lee<sup>\*,†,¶,||</sup>

<sup>†</sup>Department of Food Science, Cornell University, Ithaca, New York 14850, United States

<sup>‡</sup>Functional Food Center, Korea Institute of Science and Technology (KIST), Daejeon-dong, Gangneung 210-340, Republic of Korea

<sup>§</sup>Department of Agricultural Biotechnology, Seoul National University, Seoul 151-742, Republic of Korea

**ABSTRACT:** This study explored whether chlorogenic acid (CGA) and coffee have protective effects against retinal degeneration. Under hypoxic conditions, the viability of transformed retinal ganglion (RGC-5) cells was significantly reduced by treatment with the nitric oxide (NO) donor *S*-nitroso-*N*-acetylpenicillamine (SNAP). However, pretreatment with CGA attenuated cell death in a concentration-dependent manner. In addition, CGA prevented the up-regulation of apoptotic proteins such as Bad and cleaved caspase-3. Similar beneficial effects of both CGA and coffee extracts were observed in mice that had undergone an optic nerve crush (ONC) procedure. CGA and coffee extract reduced cell death by preventing the down-regulation of Thy-1. Our *in vitro* and *in vivo* studies demonstrated that coffee and its major component, CGA, significantly reduce apoptosis of retinal cells induced by hypoxia and NO, and that coffee consumption may help in preventing retinal degeneration.

**KEYWORDS:** coffee, chlorogenic acid, neuroprotection, retinal degeneration, hypoxia, RGC-5, glaucoma

### ■ INTRODUCTION

The retina, a thin layer of tissue on the inside back wall of the eye, contains millions of light-sensitive cells and other nerve cells that receive and organize visual information. Collectively, these cells send visual information to the brain through the optic nerve. The retina is one of the most metabolically active tissues in the body, consuming oxygen more rapidly than any other tissues, including the brain. Therefore, it is susceptible to a variety of diseases caused by oxidative stress, including age-related macular degeneration, diabetic retinopathy, and glaucoma—all of which can lead to partial or complete blindness.<sup>1</sup>

One mechanism of retinal degeneration is hypoxia, a reduction in retinal oxygen supply caused by pathologies such as central retinal artery occlusion, ischemic central retinal vein thrombosis, complications of diabetic eye disease, and some types of glaucoma that cause vascular eye diseases.<sup>2,3</sup> Retinal hypoxia can negatively impact both tissue function and cell viability, and is a potential risk factor for sight-threatening disorders.<sup>4</sup>

Unsurprisingly, there has been great interest in identifying neuroprotective compounds that inhibit hypoxia. Particularly promising in this capacity are natural products and phytochemicals that act as antioxidants and can be taken regularly without causing significant side effects.<sup>5–7</sup>

One important group of neuroprotectants comprises derivatives of chlorogenic acid (CGA). Collectively, these phenolic phytochemicals are known to have hepatoprotective, antibacterial, anti-inflammatory, DNA protective, and anti-cancer activities, among others.<sup>8–13</sup> Several studies have also suggested that the antioxidant properties of CGA make it a powerful neuroprotectant.<sup>14–16</sup>

CGA derivatives are found in a variety of edible plants, including tea, fruits, and vegetables. However, the major source of CGA intake in humans is coffee.<sup>17</sup> CGA is 4–12% of raw coffee, while a 200 mL cup of prepared coffee contains 200 mg of total CGA.<sup>18,19</sup> It has also been reported that part of CGA from foods enters into the blood circulation with relatively high absorption rate (33%) in the small intestine of humans.<sup>20</sup> There are also many reports for the bioavailability and pharmacokinetic profile of CGA after coffee consumption.<sup>21–23</sup> Previous studies by Farah et al. showed that major CGA compounds from green coffee are highly absorbed and metabolized in humans by a different manner throughout the whole gastrointestinal tract.<sup>22</sup>

Coffee consumption appears to decrease the risk of developing chronic diseases such as Parkinson's, prostate cancer, and diabetes.<sup>24–27</sup> It also reduces the extent of cognitive declines associated with aging.<sup>28–30</sup> The latter pattern, in particular, supports the idea that the neuroprotective effects of CGA derivatives stem from their antioxidant activities.

Despite these generally positive results, the effects of coffee consumption on ocular health are not yet clear. In particular, clinical studies on the relationship between coffee consumption and risk of glaucoma have yielded conflicting results.<sup>31,32</sup> Thus, we designed the current study to investigate whether coffee and, in particular, its main polyphenol, CGA has protective effects against the degeneration of retinal ganglion cells (RGC-5), both *in vitro* and *in vivo*.

**Received:** October 16, 2013

**Revised:** November 26, 2013

**Accepted:** December 2, 2013

**Published:** December 2, 2013

## MATERIALS AND METHODS

**Chemicals.** Hoechst 33342 and propidium iodide (PI) were purchased from Molecular Probes (Eugene, OR, USA). Fluorogold was purchased from Invitrogen (Carlsbad, CA, USA). Anticleaved caspase-3, anti-Bad, and anti-Thy-1 were purchased from Cell Signaling Technology (Danvers, MA, USA). Anti- $\beta$ -actin and secondary antibodies were purchased from Santa Cruz Biotechnology (Santa Cruz, CA, USA).

The VECTASHIELD Mounting Medium was purchased from Vector Laboratories (Burlingame, CA, USA). Zoletil and Rumpun were used as anesthesia and purchased from Virbac Laboratories (Fort Worth, TX, USA) and Bayer (Newbury, UK), respectively.

Chlorogenic acid (C3878) and all other chemicals and reagents were purchased from Sigma-Aldrich (St. Louis, MO, USA).

**Animals.** All animal studies were carried out in a pathogen-free barrier zone at the KIST Gangneung Institute and were done in accordance with the procedure outlined in the Association for Research in Vision and Ophthalmology (ARVO) Statement for the Use of Animals in Ophthalmic and Vision Research. Procedures used in this study were approved by the Animal Care and Use Committee of KIST.

Male ICR mice weighing between 30 and 35 g (5 weeks of age) were used in the present study and were acclimated for at least one week, were caged in groups of five or less, and were fed with a diet of animal chow and water *ad lib*. They were housed at  $23 \pm 0.5$  °C and 10% humidity with a 12 h light-dark cycle.

**Preparation of the Crude Extract from Coffee Powder.** The coffee sample was obtained from a local supermarket (Colombian roast and ground coffee, Tesco, U.K.). Ground coffee (30.0 g) was refluxed with 70% EtOH (600 mL) three times each for 3 h, and the combined solution was filtered and evaporated under vacuum to give a 70% EtOH extract (9.76 g).

**HPLC Analysis.** Coffee extract (CE) was analyzed by HPLC to quantify CGA using an Agilent 1200 series system, equipped with a G1379B vacuum degasser, a G1312A binary pump, a G1329A autosampler, a G1316A column oven, and a G1315B DAD detector (Agilent, Palo Alto, CA, USA). The separation was carried out on a Shiseido MGII C-18 column (250 mm  $\times$  4.6 mm i.d., 5  $\mu$ m particle size). The mobile phase consisted of 0.1% TFA in water and acetonitrile (93:7) with a flow rate of 1.0 mL/min during 45 min. The UV detector was set at 330 nm with full spectral scanning from 200 to 400 nm, and the sample injection volume was 10  $\mu$ L.

A standard solution of CGA (31.25–1000  $\mu$ g/mL) was prepared in methanol, and 10  $\mu$ L of each was injected into the HPLC column via the autoinjector. The linearity was evaluated by linear regression analysis, which was calculated by the least-squares regression method. The limit of detection (LOD) and the lower limit of quantification (LOQ) were defined as the minimum concentration at the signal-to-noise ratio (S/N), equal to 3.3 and 10, respectively. The precision, accuracy, and recovery were evaluated by analyzing three different concentrations on the same day and on three different days. All the experiments were carried out in triplicate.

**Culture of RGC-5 Cells.** RGC-5 cells that are proven to be of mice origin are highly relevant to the study of glaucomatous neurodegeneration and have been previously shown to express ganglion cell markers and ganglion cell-like behavior in culture.<sup>33,34</sup>

To mimic physiological hypoxic stress, RGC-5 cultures were transferred into a closed hypoxic chamber (Billups-Rothenberg Inc., Del Mar, CA, USA) in which the gas levels (1% O<sub>2</sub>, 5.13% CO<sub>2</sub>, and 93.87% N<sub>2</sub>) and temperature (37 °C) were automatically controlled, and they were incubated for 24 h. Under hypoxic conditions, cells were cotreated with *S*-nitroso-*N*-acetylpenicillamine (SNAP), a nitric oxide (NO) donor, with low glucose (5.5 mM) Dulbecco's modified Eagles's medium (DMEM; Gibco, Carlsbad, CA), which mimics physiological normal blood sugar levels *in vivo*. Culture of RGC-5 cells in 96-well plates was analyzed 24 h later for cell viability, and the cells in a 60 mm<sup>2</sup> dish were analyzed 24 h later for Western blot analysis.

**Cell Viability.** To measure the relative number of living cells, an EZ cytox cell viability assay kit (Daeil Labservice, Seoul, Korea) for a WST-1 assay was used.

The number of living cells in each well was determined by measuring the optical density (OD) at 460 nm with a microplate reader (BioTek Instruments, Winooski, VT, USA). This quantity was expressed relative to the control value.

**Microscopic Analysis of Cell Viability by Hoechst 33342 and PI Double Staining.** The Hoechst 33342 and PI double staining method was used to determine whether cell death occurred as a result of apoptosis or necrosis.<sup>35</sup> The cells were stained with 8  $\mu$ M Hoechst 33342 and 1.5  $\mu$ M PI for 30 min at 37 °C. After being washed twice with serum free media, the cells were imaged using a fluorescence microscope (Olympus, Tokyo, Japan).

**Protein Extraction and Western Blot Analysis.** The cells were scraped using a cell scraper and centrifuged at 14,000g for 10 min. The cell pellets were resuspended in cell lysis buffer [1 M Tris pH 7.4, 2 M NaCl, 1 M EDTA, 10% NP40, 1  $\times$  protease inhibitors, 1 mM PMSF] and then incubated on ice for 10 min. The extracted cells were centrifuged at 14,000g for 30 min at 4 °C. The supernatant was sonicated, and the total protein concentration was determined using a Bio-Rad Protein Assay kit (Bio-Rad Laboratories, Hercules, CA, USA).

Western blot analysis was performed with the primary antibodies, including anticleaved caspase-3, anti-Bad, anti-Thy-1 (1:1000, Cell Signaling Technology, Beverly, MA, USA), and  $\beta$ -actin (1:3000, Santa Cruz Biotechnology, CA, USA). Secondary antibodies were purchased from Santa Cruz Biotechnology Co. Ltd. (1:3000, Santa Cruz Biotechnology, CA, USA). Immunoreactive bands were detected using enhanced chemiluminescence reagents (Amersham Bioscience, GE Healthcare, U.K.) and were measured via densitometry using a LAS-4000 image reader and Multi Gauge 3.1 software (Fuji Photo Film, Japan).

**Histological Analysis.** For Hematoxylin and Eosin staining, the enucleated eyes were fixed in 10% formalin for 24 h, embedded in paraffin, and sectioned through an equatorial plane at 4  $\mu$ m thickness using a HM340E microtome (Walldorf, Germany). Four sections ( $n = 4$ ) were used for analysis.

Hematoxylin solution was added to the retina section (0.1% hematoxylin, 10% ammonium) for 8 min. The sections were then washed three times with distilled water. Bluing reagent (0.2% lithium carbonate solution) was added to the section for 1 min. The sections were quickly rinsed in 95% alcohol, and 1% Eosin Y solution was added to the sections for 1 min. Eosin Y was washed off with 95% alcohol three times, and the sections were cover-slipped with a mounting medium and observed under a light microscope (Olympus, Tokyo, Japan).<sup>36</sup>

For TUNEL staining, the sections were submitted to enzymatic digested with 20  $\mu$ g/mL of proteinase K for 15 min and then washed with PBS and incubated with 3% hydrogen peroxide in PBS for 5 min at room temperature and twice rinsed in PBS. They were then immersed, incubated with a stock solution of terminal deoxynucleotidyl transferase (TdT) reaction enzyme in a humidified chamber at 37 °C for 1 h, and then washed three times in PBS for 1 min. The sections were subsequently incubated with antidigoxigenin peroxidase conjugate and peroxidase substrate. Histological analysis was performed with a light microscope (Olympus, Tokyo, Japan), allowing us to look for signs of apoptosis (brown staining).

**Optic Nerve Crush.** Five-week-old ICR mice with a body weight of 30–35 g were used in the study.

Animals were anaesthetized by intraperitoneal injection with a mixture of Zoletil (1.6  $\mu$ g/g, Verbac Laboratories 06515, France) and Rompun (0.05  $\mu$ L/g, Bayer), and retinal damage was induced using optic nerve crush (ONC).<sup>37</sup> The optic nerve of the left eye in all treatment groups was exposed by opening the meninges of the optic nerve with the sharp tips of a forceps, followed by blunt dissection. Then the exposed optic nerve was partially crushed 2 mm behind the globe for 10 s with a cross-action calibrated forceps. In each case, a "sham" operation was performed in the same way on the partner eye, but without closing the forceps, to check for any falsifying influence of surgery on the treatment effects. In all cases the retinal blood supply

remained grossly intact, as judged on the basis of a direct ophthalmoscopic inspection. After ONC in mice, CGA or CE was dissolved in PBS, and administered orally at a dose of 10 mg/kg and 30 mg/kg for 2 weeks once a day.

All eyeballs were enucleated immediately after mice were sacrificed, and then fixed for retrograde labeling of retinal ganglion cells (RGCs).

**RGC Labeling and Retinal Flat Mount Preparation.** Mice were anesthetized by intraperitoneal or intramuscular administration of a mixture of Zoletil (1.6  $\mu\text{g/g}$ , Verbac Laboratories 06515, France) and Rompun (0.05  $\mu\text{L/g}$ , Bayer) 9 days after CGA or CE treatment. The skin over the cranium was incised, and the scalp was exposed. Holes approximately 2 mm in diameter were drilled in the skull 4 mm posterior to the bregma, 1 mm lateral to the midline, with a dentist's drill on both sides of the midline raphe. These positions correspond to the superior colliculi as determined from a stereotactic mouse brain atlas.

The superior colliculi were exposed by gentle aspiration of the overlying occipital cortex. A piece of Gelfoam soaked in a 5% solution of the neurotracer dye Fluorogold (Invitrogen, NY, USA) was directly applied to each superior colliculus. Skull openings were then sealed with a petrolatum-based antibiotic ointment. The overlying skin was sutured and antibiotic ointment applied externally.

Five days after the application of Fluorogold (enough time to allow retrograde uptake of the dye and labeling of the RGC somata), mice were sacrificed by transcardial perfusion with 4% buffered paraformaldehyde (Sigma-Aldrich, St. Louis, MO, USA) while under the same anesthesia as that used for RGC labeling. Eyes were immediately enucleated, and the retinas were detached at the ora serrata and cut with a trephine around the optic nerve head. Four radial relaxing incisions were made and the retinas prepared as flattened whole mounts on silane-coated microscope slides.<sup>38</sup>

**Statistical Analysis.** The data are expressed as a mean percentage of the control value plus standard error of the mean (SEM). Statistical comparisons were made using a one-way ANOVA followed by a Dunnett's test. Statistical analyses were conducted using GraphPad Prism (version 4.0) (GraphPad, San Diego, CA, USA). Significance was defined as  $p < 0.05$ .

## RESULTS AND DISCUSSION

**Cell Viability Following Treatment with SNAP and/or Hypoxia.** Under normoxic conditions, we observed no changes in cell viability when RGC-5 cells were treated with SNAP (data not shown). Likewise, the two lowest concentrations of SNAP did not have any noticeable effects on the viability of RGC-5 cells exposed to hypoxic conditions (Figure 1). However, both the 50 and 100  $\mu\text{M}$  treatments resulted in

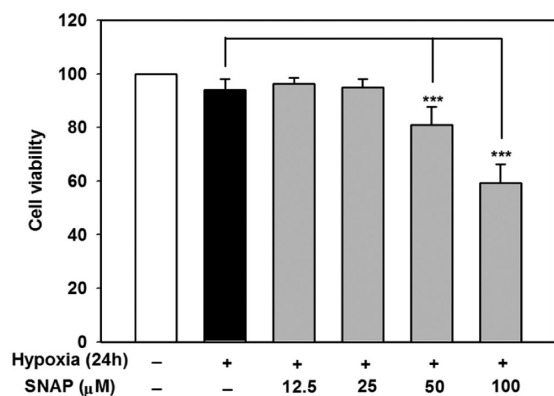


**Figure 1.** Effects of *S*-nitroso-*N*-acetylpenicillamine (SNAP) on the viability of retinal ganglion (RGC-5) cells cultured under hypoxic conditions for 24 h. Values are presented as means ( $n = 6$  independent experiments per treatment); error bars indicate SEM. Triple asterisks (\*\*\*) indicate  $p < 0.001$ .

highly significant reductions in viability ( $p < 0.001$ ). The 100  $\mu\text{M}$  treatment had a particularly noticeable effect, causing a 41% reduction of viability. Thus, this is the concentration that was used in the *in vitro* experiments (Figure 1).

The negative effects of SNAP observed here are similar to those previously reported by Sato et al. (2010).<sup>39</sup> They found that treatment with SNAP under hypoxic conditions resulted from activation of caspase and the formation of superoxide anions and peroxynitrite.<sup>39</sup>

**Cell Viability Following Treatment with SNAP and CGA.** CGA significantly blunted the negative effect of SNAP on RGC-5 cells (Figure 2). This effect was dose-dependent, with cell viability increased by 72.6%, 92.7%, and 101.6% in response to 25, 50, and 100  $\mu\text{M}$  CGA pretreatments, respectively (all  $p < 0.001$  in comparison with the control; Figure 2A).

The antioxidant *N*-acetylcysteine (NAC) and the NO scavenger 2,4-carboxyphenyl-4,4,5,5-tetramethylimidazole-1-oxyl-3-oxide (CPTIO) were used as positive controls. Both

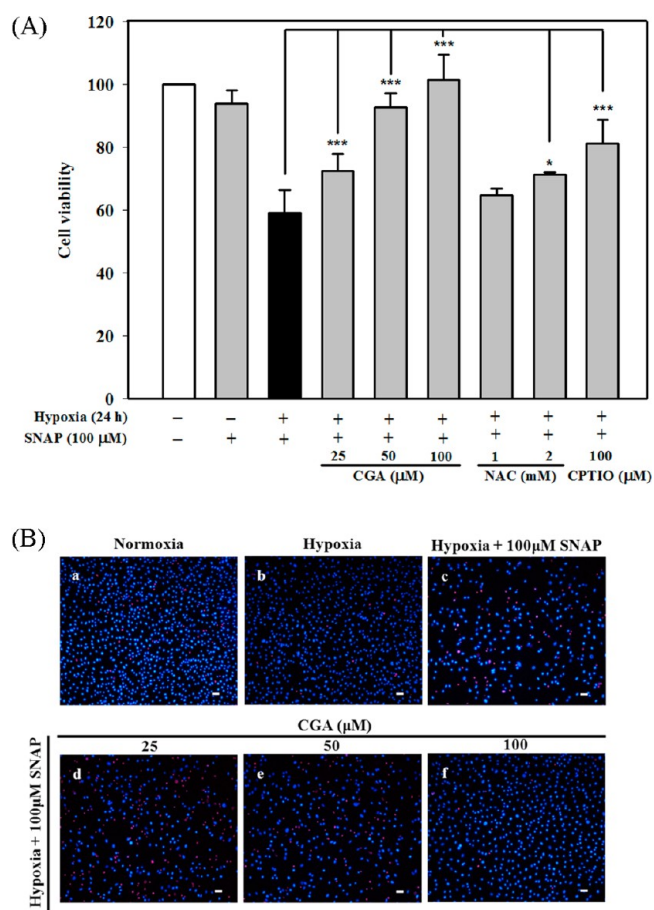


**Figure 2.** Effects of the chlorogenic acid (CGA) treatment on retinal ganglion (RGC-5) cells exposed to *S*-nitroso-*N*-acetylpenicillamine (SNAP) under hypoxic conditions. (A) Results of the WST-1 assay. Values are presented as means ( $n = 6$  independent experiments per treatment); error bars indicate SEM. Single asterisks (\*) indicate  $p < 0.05$ ; triple asterisks (\*\*\*) indicate  $p < 0.001$ . (B) Representative fluorescence microscopy of PI (red) and Hoechst 33342 (blue) staining. (a) Control RGC-5 cells under normoxic conditions. (b) RGC-5 cells under hypoxic conditions. (c) RGC-5 cells treated with 100  $\mu\text{M}$  SNAP under hypoxic conditions. (d–f) RGC-5 cells pretreated with CGA (25, 50, and 100  $\mu\text{M}$  concentrations, respectively) prior to being exposed to 100  $\mu\text{M}$  SNAP under hypoxic conditions. Scale bar = 50  $\mu\text{m}$ .

treatments also significantly reduced the negative impacts of SNAP observed in the untreated controls ( $p < 0.05$  for the 2 mM NAC treatment, and  $p < 0.001$  for the 100  $\mu\text{M}$  CPTIO treatment; Figure 2A). Previous work has shown that the benefits of CPTIO stem from its suppression of both caspase activation and NO production.<sup>39</sup> CGA has been considered an antioxidant agent; moreover, CGA is a potent inhibitor of NO production by the inhibition of the expression of inflammatory proteins such as COX-2 and iNOS, without cytotoxic effects.<sup>40,41</sup>

The similar viabilities observed in cells treated with CPTIO and CGA treatments suggest that CGA may protect cells by scavenging NO that might otherwise lead to neurodegeneration of RGC-5 cells under hypoxic conditions.

Fluorescence microscopy of Hoechst 33342- and PI-stained cells revealed similar patterns to those produced by the WST-1 assay (Figure 2B). More apoptotic/necrotic cells were observed in cultures treated with SNAP than in control cultures. However, lower levels of cell death were observed in cultures that had been pretreated with CGA; this was particularly noticeable in response to the 100  $\mu\text{M}$  CGA treatment.

Our Western blot analysis showed up-regulation of Bad and cleaved caspase-3 in cells that had been exposed to SNAP under hypoxic conditions, in relation to  $\beta$ -actin of the control (Figure 3). However, this response was noticeably suppressed in cells given a 100  $\mu\text{M}$  CGA pretreatment. A similar pattern was observed in cells treated with CPTIO as a positive control.

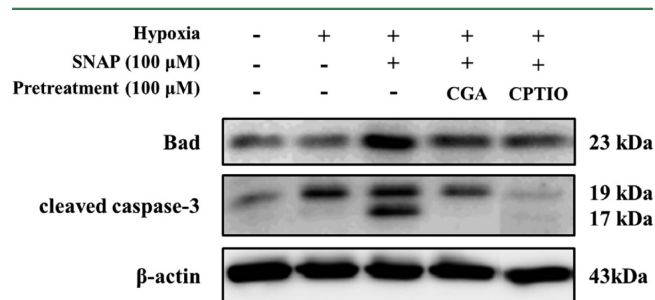


**Figure 3.** Western blot of apoptotic proteins in RGC-5 cells subjected to 100  $\mu\text{M}$  SNAP for 24 h under hypoxic conditions. The nitric oxide (NO) scavenger 2,4-carboxyphenyl-4,4,5,5-tetramethylimidazole-1-oxyl-3-oxide (CPTIO) was used as a positive control. Pretreatment with CGA appeared to have antiapoptotic effects on hypoxia and NO-induced down-regulation of both Bad and cleaved caspase-3.

Bad (BCL-2 antagonist of cell death), a pro-apoptotic protein in the BH3 domain-only group,<sup>42</sup> is the key regulator of apoptosis and is, itself, regulated primarily by phosphorylation.<sup>43,44</sup> Bad can be cleaved into a shortened form by caspases, which are cysteine proteases that play an important role in apoptosis.<sup>45–47</sup> When this cleavage occurs, Bad can be a more potent inducer of apoptosis.<sup>46,47</sup> Apoptosis is also facilitated by the activity of caspase-3, which is known to promote neuronal apoptosis.<sup>48,49</sup>

**Effects of CGA on Optic Nerve Crush-Induced Retinal Damage in Mouse.** ONC is a well-known experimental model for chronic glaucoma. During the procedure, the surgically exposed optic nerve is clamped for several seconds, resulting in both primary RGC death due to the optic nerve injury and secondary death of surrounding, uninjured RGCs.<sup>50</sup>

Results from our histological hematoxylin and eosin staining assay can be seen in Figure 4A. Relative to tissues that underwent no ONC (Figure 4A, a), those that were crushed

but received no chemical treatment exhibited a clear thinning of the inner plexiform layer (IPL) (Figure 4A, b). However, this thinning appears to have been inhibited in tissues treated with CGA (Figure 4A, c and d).

In addition to investigating these morphological patterns, we also used TUNEL staining to explore whether CGA could also reduce ganglion cell apoptosis associated with ONC (Figure 4B). Control tissues (Figure 4B, a) had fewer TUNEL-positive cells than those subjected to ONC (Figure 4B, b). As with the hematoxylin and eosin assay, however, we found that the negative effects of ONC were mitigated by treatment with CGA; in this case, there were notably fewer TUNEL-positive cells in the ganglion cell layer (GCL) of tissues treated with CGA (Figure 4B, c and d).

RGC survival was much lower in tissues that had undergone optic nerve crush (ONC) than in controls (Figure 4C, a–d). In tissues that had been treated with CGA, however, RGC survival was markedly higher (Figure 4C, e–h). This was particularly true in tissues that had been dosed with 30 mg/kg of CGA (Figure 4C, g and h). Further, both CGA treatments appeared to prevent the dramatic decrease (52.7%) in Thy-1 protein that occurred in tissues that had undergone ONC (Figure 4D). Thy-1 is a surface glycoprotein expressed uniquely in RGCs; it serves as an early marker of RGC loss in models of retinal damage.<sup>51</sup>

Indeed, 30 mg/kg CGA was similar or more effective for the neuroprotective effects on retinal degeneration than the same concentration of epigallocatechin gallate (EGCG) used as positive control; thus, the patterns reported here strongly suggest that CGA is a powerful neuroprotectant that can prevent retinal cell death.

Previously reported mechanisms for the degeneration by ONC include blockade of axonal transport resulting in inadequate supply of neurotrophic factors, disturbances of intracellular calcium homeostasis, activation of cell death genes, and local excitotoxicity due to uncontrolled activation of NMDA receptors.<sup>52,53</sup> ONC induces apoptotic cascades during which cytochrome *c* is released and both caspases-9 and -3 are subsequently activated.<sup>54,55</sup>

Injury of the optic nerve also causes an inflammatory response involving the release of cytotoxic compounds such as free radicals, NO, and glutamate.<sup>56</sup>

Administration of SNAP under hypoxic conditions has been associated with NO release, causing RGC-5 cell death by decreasing mitochondrial membrane potential, increasing the formation of superoxides, and activating caspases.<sup>39</sup> Thus, our current data suggest that the beneficial effects of CGA on retinal cells, both *in vitro* and *in vivo*, are partly due to its NO scavenging activity.

**HPLC Chromatograms of CE and Standardization of CGA in CE.** HPLC chromatograms of CE showed a CGA peak retention time at 28.5 min (Figure 5). We observed no interference from other materials in the extract, indicating that the specificity of the method was reliable. The limits of detection (LOD) and limits of quantification (LOQ) for CGA were 7.67  $\mu\text{g}/\text{mL}$  and 23.26  $\mu\text{g}/\text{mL}$ , respectively (Table 1). Precision is the measure of how close the data values are to each other for a number of measurements under the same analytical conditions and expressed as the % relative standard deviation (%RSD) of each analyte concentration. Our analyses were associated with very low levels of relative standard deviation (RSD: intraday, >2.57%; interday, >2.60%), indicating that our CGA measurements were highly precise (Table 2).

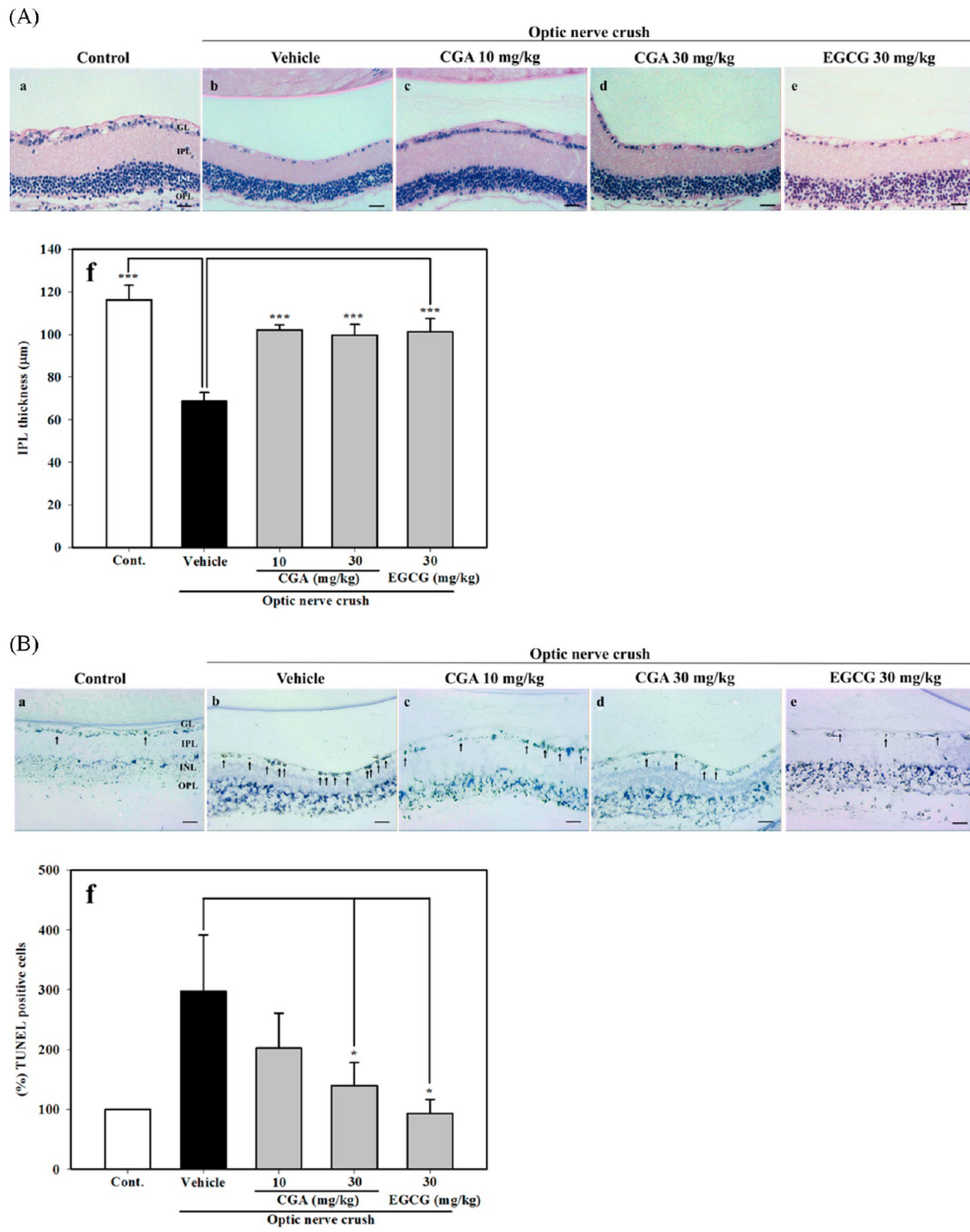
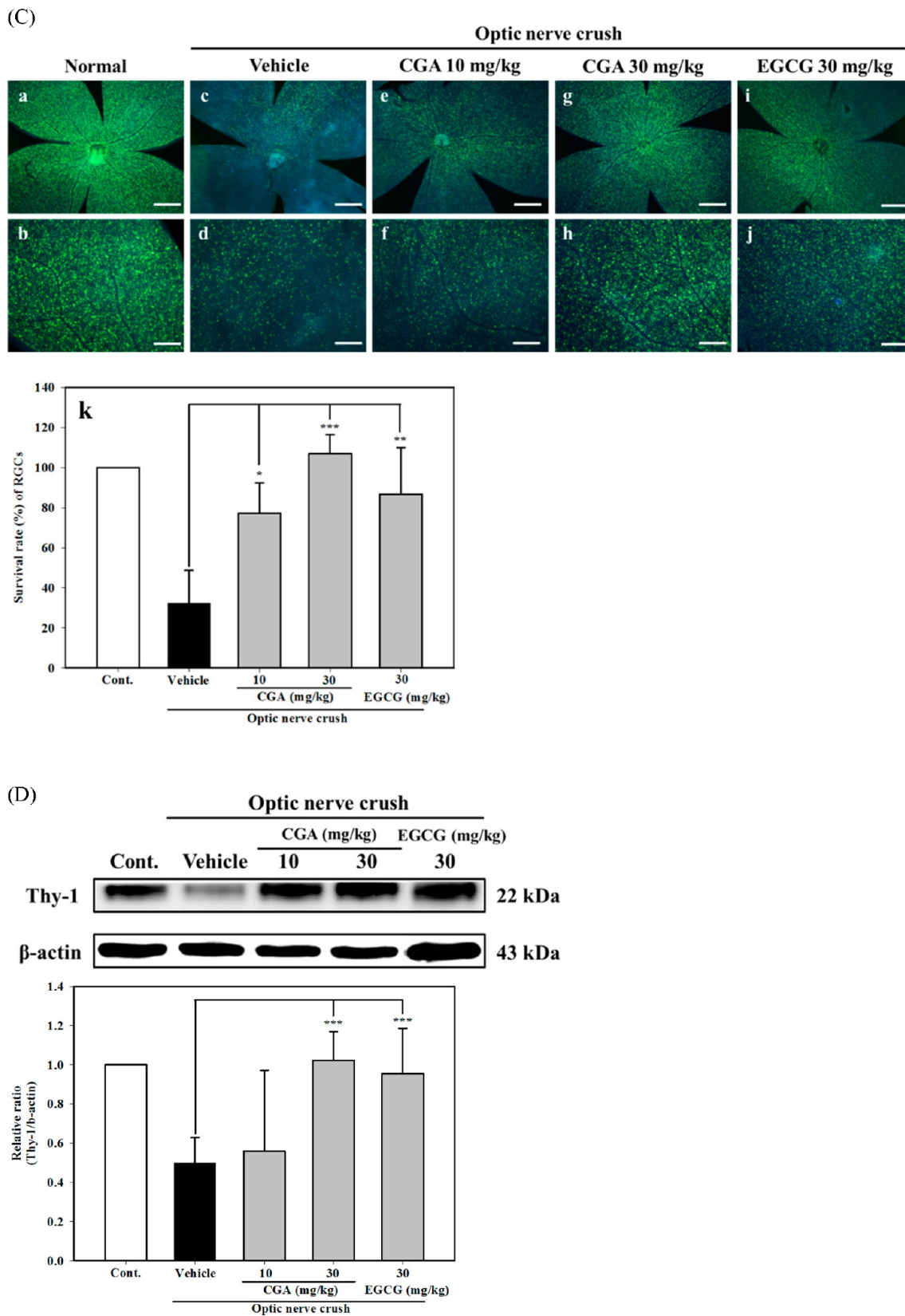


Figure 4. continued



**Figure 4.** Optic nerve crush (ONC) experiments on the impacts of a CGA treatment on retinal tissues of mice. (A) Representative photomicrographs of tissues stained with hematoxylin and eosin. Tissues from (a) a control, (b) a mouse that underwent ONC only, (c) a mouse that underwent ONC and was treated with 10 mg/kg of CGA, (d) a mouse that underwent ONC and was treated with 30 mg/kg, and (e) a mouse that underwent ONC and was treated with 30 mg/kg of epigallocatechin gallate (EGCG). The thickness of IPL (f). Results are mean values, with error bar indicating mean SEM. Triple asterisks (\*\*\*) indicate  $p < 0.001$ . (B) Representative photomicrographs of TUNEL-stained cells. Arrows indicate TUNEL-positive cells (brown stain). Scale bar = 50  $\mu$ m. The quantification of TUNEL positive cells (f). Results are mean values with error bar indicating mean SEM. Single asterisk (\*) indicates  $p < 0.05$ . (C) Representative micrographs showing Fluorogold-labeled retinal ganglion cells

Figure 4. continued

(RGCs) harvested from mice 14 days after optic nerve crush (ONC). Retina from (a) an untreated control mouse, (c) a mouse that underwent ONC only, (e) a mouse that underwent ONC and was treated with 10 mg/kg of CGA, (g) a mouse that underwent ONC and was treated with 30 mg/kg of CGA, and (i) a mouse that underwent ONC and was treated with 30 mg/kg EGCG. Images in the lower row are 100× magnifications of the images above them; scale bars in the upper row represent 500  $\mu\text{m}$ , while scale bars in the lower row represent 100  $\mu\text{m}$ . (k) Quantitative analysis of the survival (%) rate of RGCs 14 days after ONC. Experimental values are expressed as mean SEM. Single asterisks (\*) indicate  $p < 0.05$ ; double asterisks (\*\*) indicate  $p < 0.01$ ; triple asterisks (\*\*\*) indicate  $p < 0.001$ . (D) Results of Western blot analysis investigating Thy-1 expression in RGCs 14 days after the ONC procedure. Densitometric analysis of Thy-1 levels; data are shown as mean SEM. Single asterisks (\*) indicate  $p < 0.05$ .

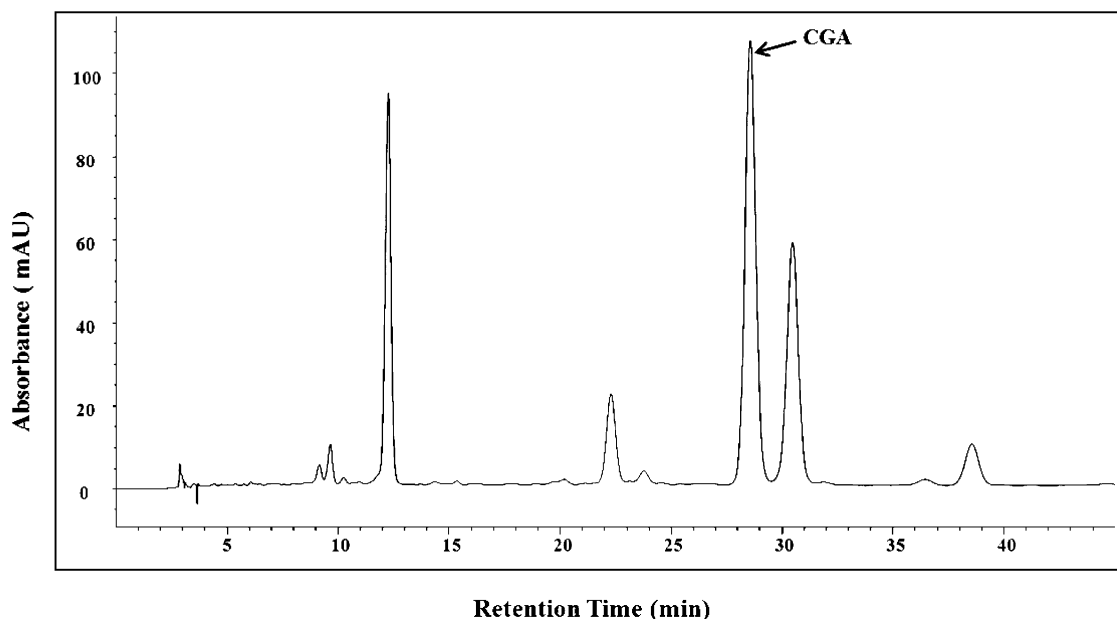


Figure 5. High-performance liquid chromatography analysis of coffee extract (prepared in 70% EtOH); ultraviolet detection was performed at 330 nm. The arrow indicates the peak corresponding to CGA.

Table 1. Calibration Curve, Correlation Coefficients, Limits of Detection (LOD), and Limits of Quantification (LOQ) of CGA

standard sample	range ( $\mu\text{g/mL}$ )	slope	intercept	$R^2$	LOD <sup>a</sup> ( $\mu\text{g/mL}$ )	LOQ <sup>a</sup> ( $\mu\text{g/mL}$ )
CGA	31.25–1000	24.226	167.56	1.0	7.67	23.26

<sup>a</sup> $n = 3$  replicates.

Table 2. Intra- and Interday Precision and Accuracy for the Determination of CGA

stand sample	conc ( $\mu\text{g/mL}$ )	intraday ( $n = 3$ )			interday ( $n = 3$ )		
		found conc ( $\mu\text{g/mL}$ ) $\pm$ SD	recovery (%)	%RSD <sup>a</sup>	found conc ( $\mu\text{g/mL}$ ) $\pm$ SD	recovery (%)	%RSD <sup>a</sup>
CGA	61.25	64.42 $\pm$ 0.94	103.07	1.46	61.60 $\pm$ 1.60	98.56	2.60
	125	126.88 $\pm$ 3.06	101.50	2.41	125.28 $\pm$ 0.45	100.22	0.36
	250	253.45 $\pm$ 6.51	101.38	2.57	246.47 $\pm$ 0.40	98.59	0.16

<sup>a</sup>RSD refers to the relative standard deviation.

The accuracy by mean recovery (%) for CGA ranged from 98.56 to 103.07% (Table 2), thus it can be accurately determined by this method from any small changes in the standard sample concentration.<sup>57</sup>

**Effects of CE on Optic Nerve Crush-Induced Retinal Damage in Mouse.** In addition to investigating the effects of pure CGA on retinal degeneration, we also explored whether CE, a major source of CGA, has similar benefits. As we observed in the CGA activity, lower levels of RGC death were found in control tissues (Figure 6A, a and b) than in those that were crushed but not treated with exogenous compounds (Figure 6A, c and d). In tissues treated with 50 mg/kg of CE, however, cell death was markedly reduced (Figure 6A, i and j).

The protective effects of CE occur in a dose-dependent manner (Figure 6A, e–j). Likewise, while the 50 mg/kg CE treatment was associated with a preservation of Thy-1 expression, the 10- and 30 mg/kg CE treatments were less effective than the group of 50 mg/kg CE treatments (Figure 6B).

Based on the HPLC chromatogram of CE, we found 14.7 mg/g of CGA in CE. Although the amount of CGA in CE is less than the reported amount, the group of CE treatment shows similar protective effects with the CGA treatments (Figures 4C and 6A).<sup>19</sup>

Since significant amounts of CGA are metabolized in the human intestine and some phenolic metabolites of coffee are known to possess high antioxidant activity,<sup>58</sup> we expect that the

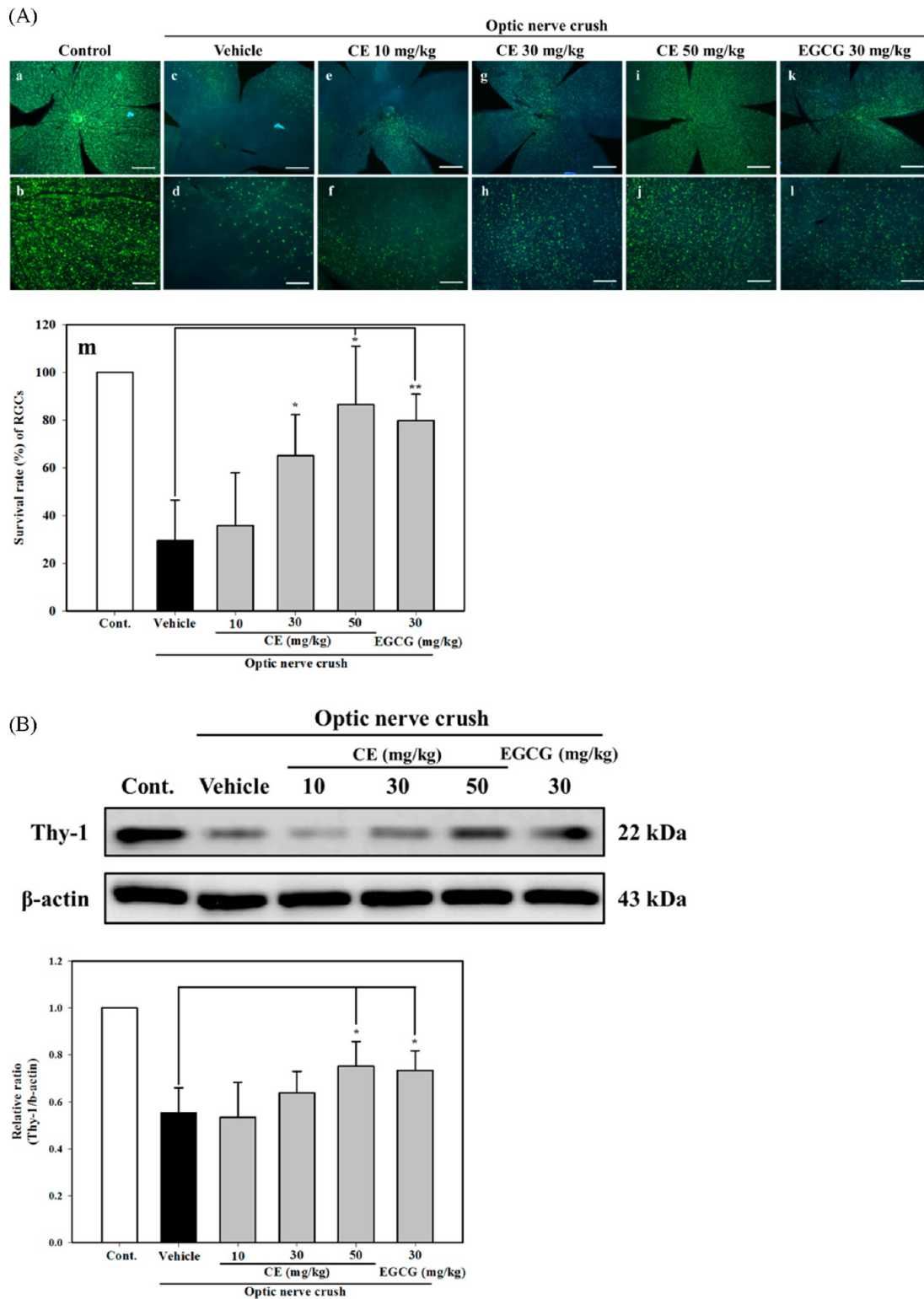


**Figure 6.** Optic nerve crush (ONC) experiments on the impacts of CE treatment on retinal tissues of mice. (A) Representative micrographs of Fluorogold-labeled tissues from (a) a control, (c) a mouse that underwent ONC, (e) a mouse that underwent ONC and was treated with 10 mg/kg of CE, (g) a mouse that underwent ONC and was treated with 30 mg/kg of CE, (i) a mouse that underwent ONC and was treated with 50 mg/kg of CE, and (k) a mouse that underwent ONC and was treated with 30 mg/kg EGCG. Images in the lower row are 100 $\times$  magnifications of the images in the row above them; scale bars in the upper row represent 500  $\mu$ m, while scale bars in the lower row represent 100  $\mu$ m. (m) Quantitative analyses of the survival (%) rate of RGCs 14 days after ONC. Experimental values are expressed as mean SEM. Single asterisks (\*) indicate  $p < 0.05$ ; double asterisks (\*\*) indicate  $p < 0.01$ . (B) Results of Western blot analysis investigating Thy-1 expression in RGCs 14 days after the ONC procedure. Densitometric analysis of Thy-1 levels; data are shown as mean SEM. Single asterisks (\*) indicate  $p < 0.05$ .

additional bioactivities are originated from those metabolites. Therefore, the research on the protective effects of CGA and coffee metabolites on retina is being conducted.

In conclusion, this study shows that CGA and coffee extract are responsible for reduction of the RGC apoptosis induced by hypoxia and NO. Therefore, coffee consumption may provide additional health benefits by preventing retinal degeneration.

## AUTHOR INFORMATION

### Corresponding Authors

\*E-mail: shjung507@gmail.com. Phone: +82-33-650-3653. Fax: +82-33-650-3679.

\*E-mail: cyl1@cornell.edu. Phone: +1-607-255-0114. Fax: +1-607-254-4868.

### Author Contributions

<sup>†</sup>S.H.J. and C.Y.L. equally contributed to this article.

### Funding

This work was financially supported by an intramural grant (2Z03943, 2Z03850) from the Korea Institute of Science and Technology (KIST), Republic of Korea.

### Notes

The authors declare no competing financial interest.

## ACKNOWLEDGMENTS

The RGC-5 cells were a generous gift from Alcon Research, Ltd.

## ABBREVIATIONS

SNAP, S-nitroso-N-acetyl-DL-penicillamine; ONC, optic nerve crush; CGA, chlorogenic acid; CE, coffee extract; LOD, limit of detection; LOQ, limit of quantification; RGC, retinal ganglion cell; IOP, intraocular pressure; DCFH-DA, dichlorofluorescein diacetate; PI, propidium iodide; ARVO, Association for Research in Vision and Ophthalmology; HPLC, high-performance liquid chromatography; CPTIO, 2,4-carboxyphenyl-4,4,5,5-tetramethylimidazole-1-oxyl-3-oxide; IPL, inner plexiform layer; GCL, ganglion cell layer; DMEM, Dulbecco's modified Eagle's medium; FBS, fetal bovine serum; NMDA, N-methyl-D-aspartate; NAC, N-acetyl-L-cysteine; NO, nitric oxide; DMSO, dimethyl sulfoxide; ROS, reactive oxygen species; PMSF, phenylmethylsulfonyl fluoride; PVDF, polyvinylidene difluoride; TdT, terminal deoxynucleotidyl transferase; TUNEL, terminal deoxynucleotidyl transferase dUTP nick end labeling; SEM, standard error of the mean; COX-2, cyclooxygenase-2; iNOS, inducible nitric oxide synthase

## REFERENCES

- (1) Ames, A. Energy requirements of CNS cells as related to their function and to their vulnerability to ischemia - a commentary based on studies on retina. *Can. J. Physiol. Pharmacol.* **1992**, *70*, S158–S164.
- (2) Levin, L. A. Retinal ganglion cells and neuroprotection for glaucoma. *Surv. Ophthalmol.* **2003**, *48* (Suppl 1), S21–24.
- (3) Sennlaub, F.; Courtois, Y.; Goureau, O. Inducible nitric oxide synthase mediates retinal apoptosis in ischemic proliferative retinopathy. *J. Neurosci.* **2002**, *22*, 3987–3993.
- (4) Kaur, C.; Foulds, W. S.; Ling, E. A. Hypoxia-ischemia and retinal ganglion cell damage. *Clin. Ophthalmol.* **2008**, *2*, 879–889.
- (5) Mozaffarieh, M.; Grieshaber, M. C.; Orgul, S.; Flammer, J. The potential value of natural antioxidative treatment in glaucoma. *Surv. Ophthalmol.* **2008**, *53*, 479–505.
- (6) Losso, J. N.; Bawadi, H. A. Hypoxia inducible factor pathways as targets for functional foods. *J. Agric. Food Chem.* **2005**, *53*, 3751–3768.

- (7) Lu, K. T.; Chiou, R. Y. Y.; Chen, L. G.; Chen, M. H.; Tseng, W. T.; Hsieh, H. T.; Yang, Y. L. Neuroprotective effects of resveratrol on cerebral ischemia-induced neuron loss mediated by free radical scavenging and cerebral blood flow elevation. *J. Agric. Food Chem.* **2006**, *54*, 3126–3131.

- (8) Henry-Vitrac, C.; Ibarra, A.; Roller, M.; Merillon, J. M.; Vitrac, X. Contribution of chlorogenic acids to the inhibition of human hepatic glucose-6-phosphatase activity in vitro by Svetol, a standardized decaffeinated green coffee extract. *J. Agric. Food Chem.* **2010**, *58*, 4141–4144.

- (9) Lou, Z.; Wang, H.; Zhu, S.; Ma, C.; Wang, Z. Antibacterial activity and mechanism of action of chlorogenic acid. *J. Food Sci.* **2011**, *76*, M398–403.

- (10) Belkaid, A.; Currie, J. C.; Desgagnes, J.; Annabi, B. The chemopreventive properties of chlorogenic acid reveal a potential new role for the microsomal glucose-6-phosphate translocase in brain tumor progression. *Cancer Cell Int.* **2006**, *6*, 7.

- (11) dos Santos, M. D.; Almeida, M. C.; Lopes, N. P.; de Souza, G. E. Evaluation of the anti-inflammatory, analgesic and antipyretic activities of the natural polyphenol chlorogenic acid. *Biol. Pharm. Bull.* **2006**, *29*, 2236–2240.

- (12) Bouayed, J.; Rammal, H.; Dicko, A.; Younos, C.; Soulimani, R. Chlorogenic acid, a polyphenol from *Prunus domestica* (Mirabelle), with coupled anxiolytic and antioxidant effects. *J. Neurol. Sci.* **2007**, *262*, 77–84.

- (13) Xu, J.-G.; Hu, Q.-P.; Liu, Y. Antioxidant and DNA-protective activities of chlorogenic acid isomers. *J. Agric. Food Chem.* **2012**, *60*, 11625–11630.

- (14) Sato, Y.; Itagaki, S.; Kurokawa, T.; Ogura, J.; Kobayashi, M.; Hirano, T.; Sugawara, M.; Iseki, K. In vitro and in vivo antioxidant properties of chlorogenic acid and caffeic acid. *Int. J. Pharm.* **2011**, *403*, 136–138.

- (15) Lee, K.; Lee, J. S.; Jang, H. J.; Kim, S. M.; Chang, M. S.; Park, S. H.; Kim, K. S.; Bae, J.; Park, J. W.; Lee, B.; Choi, H. Y.; Jeong, C. H.; Bu, Y. Chlorogenic acid ameliorates brain damage and edema by inhibiting matrix metalloproteinase-2 and 9 in a rat model of focal cerebral ischemia. *Eur. J. Pharmacol.* **2012**, *689*, 89–95.

- (16) Kim, J.; Lee, S.; Shim, J.; Kim, H. W.; Kim, J.; Jang, Y. J.; Yang, H.; Park, J.; Choi, S. H.; Yoon, J. H.; Lee, K. W.; Lee, H. J. Caffeinated coffee, decaffeinated coffee, and the phenolic phytochemical chlorogenic acid up-regulate NQO1 expression and prevent H<sub>2</sub>O<sub>2</sub>-induced apoptosis in primary cortical neurons. *Neurochem. Int.* **2012**, *60*, 466–474.

- (17) Clifford, M. N. Chlorogenic acids and other cinnamates - nature, occurrence, dietary burden, absorption and metabolism. *J. Sci. Food Agric.* **2000**, *80*, 1033–1043.

- (18) Matei, M. F.; Jaiswal, R.; Kuhnert, N. Investigating the chemical changes of chlorogenic acids during coffee brewing: conjugate addition of water to the olefinic moiety of chlorogenic acids and their quinides. *J. Agric. Food Chem.* **2012**, *60*, 12105–12115.

- (19) Farah, A.; de Paulis, T.; Moreira, D. P.; Trugo, L. C.; Martin, P. R. Chlorogenic acids and lactones in regular and water-decaffeinated arabica coffees. *J. Agric. Food Chem.* **2006**, *54*, 374–381.

- (20) Olthof, M. R.; Hollman, P. C.; Katan, M. B. Chlorogenic acid and caffeic acid are absorbed in humans. *J. Nutr.* **2001**, *131*, 66–71.

- (21) Monteiro, M.; Farah, A.; Perrone, D.; Trugo, L. C.; Donangelo, C. Chlorogenic acid compounds from coffee are differentially absorbed and metabolized in humans. *J. Nutr.* **2007**, *137*, 2196–2201.

- (22) Farah, A.; Monteiro, M.; Donangelo, C. M.; Lafay, S. Chlorogenic acids from green coffee extract are highly bioavailable in humans. *J. Nutr.* **2008**, *138*, 2309–2315.

- (23) Erk, T.; Williamson, G.; Renouf, M.; Marmet, C.; Steiling, H.; Dionisi, F.; Barron, D.; Melcher, R.; Richling, E. Dose-dependent absorption of chlorogenic acids in the small intestine assessed by coffee consumption in ileostomists. *Mol. Nutr. Food Res.* **2012**, *56*, 1488–1500.

- (24) Ross, G. W.; Abbott, R. D.; Petrovitch, H.; Morens, D. M.; Grandinetti, A.; Tung, K. H.; Tanner, C. M.; Masaki, K. H.; Blanchette, P. L.; Curb, J. D.; Popper, J. S.; White, L. R. Association

of coffee and caffeine intake with the risk of Parkinson disease. *JAMA* **2000**, *283*, 2674–2679.

(25) van Dam, R. M.; Hu, F. B. Coffee consumption and risk of type 2 diabetes - a systematic review. *JAMA* **2005**, *294*, 97–104.

(26) Wilson, K. M.; Kasperzyk, J. L.; Rider, J. R.; Kenfield, S.; van Dam, R. M.; Stampfer, M. J.; Giovannucci, E.; Mucci, L. A. Coffee consumption and prostate cancer risk and progression in the Health Professionals Follow-up Study. *J. Natl. Cancer Inst.* **2011**, *103*, 876–884.

(27) Higdon, J. V.; Frei, B. Coffee and health: a review of recent human research. *Crit. Rev. Food Sci. Nutr.* **2006**, *46*, 101–123.

(28) van Gelder, B. M.; Buijsse, B.; Tijhuis, M.; Kalmijn, S.; Giampaoli, S.; Nissinen, A.; Kromhout, D. Coffee consumption is inversely associated with cognitive decline in elderly European men: the FINE Study. *Eur. J. Clin. Nutr.* **2007**, *61*, 226–232.

(29) Shukitt-Hale, B.; Miller, M.; Chu, Y.-F.; Lyle, B.; Joseph, J. Coffee, but not caffeine, has positive effects on cognition and psychomotor behavior in aging. *Age (Dordrecht, Neth.)* **2013**, *1*–10.

(30) Chu, Y.-F.; Brown, P. H.; Lyle, B. J.; Chen, Y.; Black, R. M.; Williams, C. E.; Lin, Y.-C.; Hsu, C. W.; Cheng, I. H. Roasted coffees high in lipophilic antioxidants and chlorogenic acid lactones are more neuroprotective than green coffees. *J. Agric. Food Chem.* **2009**, *57*, 9801–9808.

(31) Pasquale, L. R.; Wiggs, J. L.; Willett, W. C.; Kang, J. H. The relationship between caffeine and coffee consumption and exfoliation glaucoma or glaucoma suspect: a prospective study in two cohorts. *Invest. Ophthalmol. Vis. Sci.* **2012**, *53*, 6427–6433.

(32) Jiwani, A. Z.; Rhee, D. J.; Brauner, S. C.; Gardiner, M. F.; Chen, T. C.; Shen, L. Q.; Chen, S. H.; Grosskreutz, C. L.; Chang, K. K.; Kloek, C. E.; Greenstein, S. H.; Borboli-Gerogiannis, S.; Pasquale, D. L.; Chaudhry, S.; Loomis, S.; Wiggs, J. L.; Pasquale, L. R.; Turalba, A. V. Effects of caffeinated coffee consumption on intraocular pressure, ocular perfusion pressure, and ocular pulse amplitude: a randomized controlled trial. *Eye (London)* **2012**, *26*, 1122–1130.

(33) Krishnamoorthy, R. R.; Agarwal, P.; Prasanna, G.; Vopat, K.; Lambert, W.; Sheedlo, H. J.; Pang, I. H.; Shade, D.; Wordinger, R. J.; Yorio, T.; Clark, A. F.; Agarwal, N. Characterization of a transformed rat retinal ganglion cell line. *Brain Res. Mol. Brain Res.* **2001**, *86*, 1–12.

(34) Van Bergen, N. J.; Wood, J. P. M.; Chidlow, G.; Trounce, I. A.; Casson, R. J.; Ju, W. K.; Weinreb, R. N.; Crowston, J. G. Recharacterization of the RGC-5 retinal ganglion cell line. *Invest. Ophthalmol. Vis. Sci.* **2009**, *50*, 4267–4272.

(35) Jung, S. H.; Kim, B. J.; Lee, E. H.; Osborne, N. N. Isoquercitrin is the most effective antioxidant in the plant *Thuja orientalis* and able to counteract oxidative-induced damage to a transformed cell line (RGC-5 cells). *Neurochem. Int.* **2010**, *57*, 713–721.

(36) Matsunaga, N.; Imai, S.; Inokuchi, Y.; Shimazawa, M.; Yokota, S.; Araki, Y.; Hara, H. Bilberry and its main constituents have neuroprotective effects against retinal neuronal damage in vitro and in vivo. *Mol. Nutr. Food Res.* **2009**, *53*, 869–877.

(37) Li, Y.; Schlamp, C. L.; Nickells, R. W. Experimental induction of retinal ganglion cell death in adult mice. *Invest. Ophthalmol. Vis. Sci.* **1999**, *40*, 1004–1008.

(38) Danias, J.; Lee, K. C.; Zamora, M. F.; Chen, B.; Shen, F.; Filippopoulos, T.; Su, Y. L.; Goldblum, D.; Podos, S. M.; Mittag, T. Quantitative analysis of retinal ganglion cell (RGC) loss in aging DBA/2N<sup>nia</sup> glaucomatous mice: Comparison with RGC loss in aging C57/BL6 mice. *Invest. Ophthalmol. Vis. Sci.* **2003**, *44*, 5151–5162.

(39) Sato, T.; Oku, H.; Tsuruma, K.; Katsumura, K.; Shimazawa, M.; Hara, H.; Sugiyama, T.; Ikeda, T. Effect of hypoxia on susceptibility of RGC-5 cells to nitric oxide. *Invest. Ophthalmol. Vis. Sci.* **2010**, *51*, 2575–86.

(40) Hwang, S. J.; Kim, Y. W.; Park, Y.; Lee, H. J.; Kim, K. W. Anti-inflammatory effects of chlorogenic acid in lipopolysaccharide-stimulated RAW 264.7 cells. *Inflamm. Res.* **2013**, *1*–10.

(41) Mullen, W.; Nemzer, B.; Stalmach, A.; Ali, S.; Combet, E. Polyphenolic and hydroxycinnamate contents of whole coffee fruits from china, India, and Mexico. *J. Agric. Food Chem.* **2013**, *61*, S298–S309.

(42) Huang, D. C.; Strasser, A. BH3-Only proteins-essential initiators of apoptotic cell death. *Cell* **2000**, *103*, 839–842.

(43) Franke, T. F.; Cantley, L. C. Apoptosis. A Bad kinase makes good. *Nature* **1997**, *390*, 116–117.

(44) Gross, A.; McDonnell, J. M.; Korsmeyer, S. J. BCL-2 family members and the mitochondria in apoptosis. *Genes Dev.* **1999**, *13*, 1899–1911.

(45) Cohen, G. M. Caspases: the executioners of apoptosis. *Biochem. J.* **1997**, *326* (Pt 1), 1–16.

(46) Fujita, N.; Nagahashi, A.; Nagashima, K.; Rokudai, S.; Tsuruo, T. Acceleration of apoptotic cell death after the cleavage of Bcl-XL protein by caspase-3-like proteases. *Oncogene* **1998**, *17*, 1295–1304.

(47) Condorelli, F.; Salomoni, P.; Cotteret, S.; Cesi, V.; Srinivasula, S. M.; Alnemri, E. S.; Calabretta, B. Caspase cleavage enhances the apoptosis-inducing effects of BAD. *Mol. Cell. Biol.* **2001**, *21*, 3025–3036.

(48) Keane, R. W.; Srinivasan, A.; Foster, L. M.; Testa, M. P.; Ord, T.; Nonner, D.; Wang, H. G.; Reed, J. C.; Bredesen, D. E.; Kayalar, C. Activation of CPP32 during apoptosis of neurons and astrocytes. *J. Neurosci. Res.* **1997**, *48*, 168–180.

(49) Kuida, K.; Zheng, T. S.; Na, S.; Kuan, C.; Yang, D.; Karasuyama, H.; Rakic, P.; Flavell, R. A. Decreased apoptosis in the brain and premature lethality in CPP32-deficient mice. *Nature* **1996**, *384*, 368–372.

(50) Levkovitch-Verbin, H.; Quigley, H. A.; Kerrigan-Baumrind, L. A.; D'Anna, S. A.; Kerrigan, D.; Pease, M. E. Optic nerve transection in monkeys may result in secondary degeneration of retinal ganglion cells. *Invest. Ophthalmol. Vis. Sci.* **2001**, *42*, 975–982.

(51) Huang, W.; Fileta, J.; Guo, Y.; Grosskreutz, C. L. Down-regulation of Thy1 in retinal ganglion cells in experimental glaucoma. *Curr. Eye Res.* **2006**, *31*, 265–271.

(52) Kreutz, M. R.; Seidenbecher, C. I.; Sabel, B. A. Molecular plasticity of retinal ganglion cells after partial optic nerve injury. *Restor. Neurol. Neurosci.* **1999**, *14*, 127–134.

(53) Schuettauf, F.; Rejdak, R.; Thaler, S.; Bolz, S.; Lehaci, C.; Mankowska, A.; Zarnowski, T.; Junemann, A.; Zagorski, Z.; Zrenner, E.; Grieb, P. Citicoline and lithium rescue retinal ganglion cells following partial optic nerve crush in the rat. *Exp. Eye Res.* **2006**, *83*, 1128–1134.

(54) Kermer, P.; Klocker, N.; Labes, M.; Thomsen, S.; Srinivasan, A.; Bahr, M. Activation of caspase-3 in axotomized rat retinal ganglion cells in vivo. *FEBS Lett.* **1999**, *453*, 361–364.

(55) Kermer, P.; Ankerhold, R.; Klocker, N.; Krajewski, S.; Reed, J. C.; Bahr, M. Caspase-9: involvement in secondary death of axotomized rat retinal ganglion cells in vivo. *Brain Res. Mol. Brain Res.* **2000**, *85*, 144–150.

(56) Maghariou, M.; D'Onofrio, P. M.; Hollander, A.; Zhu, P.; Chen, J.; Koeberle, P. D. Quantitative iTRAQ analysis of retinal ganglion cell degeneration after optic nerve crush. *J. Proteome Res.* **2011**, *10*, 3344–3362.

(57) Lim, S. S.; Lee, M. Y.; Ahn, H. R.; Choi, S. J.; Lee, J. Y.; Jung, S. H. Preparative isolation and purification of antioxidative diarylheptanoid derivatives from *Alnus japonica* by high-speed counter-current chromatography. *J. Sep. Sci.* **2011**, *34*, 3344–3352.

(58) Gomez-Ruiz, J. A.; Leake, D. S.; Ames, J. M. In vitro antioxidant activity of coffee compounds and their metabolites. *J. Agric. Food Chem.* **2007**, *55*, 6962–6969.